DOI: 10.1002/ejic.200600912

Synthesis of Tin(II) Phosphate Open Frameworks Using Isomers of 1,2-Diaminocyclohexane as Template

Xuejun Yuan,[a,b] Yi-Zhi Li,[b] Yan Xu,[b] Xiaozeng You,*[b] and Robert J. Linhardt*[a]

Keywords: Tin(II) phosphate / Open framework / Templated hydrothermal synthesis / Leaching

A novel layered framework of tin(II) phosphate, $[Sn_4(PO_4)_3(OH)]^{2-}\cdot[trans\text{-}1,2\text{-}C_6H_{10}(NH_3)_2]^{2+}$, has been synthesized under hydrothermal conditions with tin(II) oxalate, phosphoric acid and a mixture of *trans*- and *cis*-1,2-diaminocyclohexane (1,2-DACH). The compound crystallizes in the monoclinic space group $P2_1/n$ (No. 14). The channels of the *trans*-1,2-DACH are occluded by hydrogen bonding in the doubly protonated form, which is leached out from the framework. Reaction using only *tran*-DACH gives the same compound. For comparison, when *cis*-DACH is used as template under the same conditions instead of the mixture of *trans* and *cis* isomers, the neutral inorganic phosphate framework $(Sn_3O)_2(Sn_2O)_2(PO_4)_4$ is formed. It crystallizes in the triclinic space group $P\bar{1}$ (No. 2). These results suggest that *trans*-1,2-DACH is selectively occluded in the framework $[Sn_4(PO_4)_3(OH)]^{2-}\cdot[trans\text{-}1,2\text{-}C_6H_{10}(NH_3)_2]^{2+}$.
(© Wiley-VCH Verlag GmbH & Co. KGaA, 69451 Weinheim, Germany, 2007)

Introduction

During the past decade, preparation of open-framework metal phosphates has attracted much attention because of their potential applications, which take advantage of microporosity, thermal stability, appropriate acidity and their sturdiness with regard to solvent.[1] The use of structure-directing agents (SDA) or template agents in the synthesis of new solids exhibiting open-framework structures has gained prominence. It is now well established that for the synthesis of such new micro- and mesoporous materials, an organic template can be used to steer the process of crystallization to form open architectures.[2] An organic moiety is normally accommodated within the cavities or between neighboring sheets. In many cases, template can be removed by post-synthesis treatment such as calcination or chemical extraction (i.e. leaching).[3]

Open-framework tin(II) phosphate compounds can be synthesized with the aid of organic amines.[4] The building units in these compounds are commonly trigonal-pyramidal SnO_3, and/or square-pyramidal SnO_4 and tetrahedral PO_4 groups linked by sharing their vertices to form frameworks with channels and or cages.[5] The tin atoms are coordinated with oxygen atoms which occupy the vertex of pyramid, whereas the lone pair presumably occupies the fourth vertex of a polyhedron formed by oxygen atoms and the lone pair itself around the Sn^{II} atom.[6] A single organic amine quite often affords several open framework phosphates with different structures.[7] The amine might act as a structure-directing agent or merely fill the available voids and stabilize the structure through hydrogen bonding and or other interactions.[8] Because the amine generally is protonated in reactions, it also helps in charge compensation of the inorganic framework. Recently, it has been suggested the formation of the amine phosphates may act as intermediates in the formation of the metal phosphates.[8,9]

We attempted to synthesize tin(II) phosphate framework under hydrothermal conditions using a mixture of *trans*- and *cis*-1,2-diaminocyclohexane(1,2-DACH), or only *trans*-1,2-DACH, or only *cis*-1,2-DACH as template. Interestingly, two tin(II) phosphate frameworks with unique structure characteristics, $[Sn_4(PO_4)_3(OH)]^{2-}\cdot[trans\text{-}1,2\text{-}C_6H_{10}(NH_3)_2]^{2+}$ (**1**) and $(Sn_3O)_2(Sn_2O)(PO_4)_4$ (**2**), were obtained. Here, we present the syntheses and structural determinations of them. In addition, the separation of the organic amine isomers of **1** is also described.

Results and Discussion

Synthesis

Dispersion of SnC_2O_4 in aqueous phosphoric acid followed by the addition of a mixture of *trans*- and *cis*-1,2-DACH and heating under pressure at 443 K affords colorless schistose single crystals of **1**. A reaction using only *trans*-1,2-DACH under the same conditions also gives compound **1**. Synthesis utilizing only *cis*-1,2-DACH affords colorless prismatic crystals of **2**.

[a] Department of Chemistry and Chemical Biology, Rensselaer Polytechnic Institute,
Troy, NY 12180, USA
Fax: +1-518-276-3405
E-mail: linhar@rpi.edu
[b] State Key Laboratory of Coordination Chemistry, School of Chemistry and Chemical Engineering, Nanjing University,
Nanjing 210093, China
Fax: +86-25-83314502
E-mail: youxz@nju.edu.cn

 InterScience © 2007 Wiley-VCH Verlag GmbH & Co. KGaA, Weinheim

Characterization

Inductively coupled plasma (ICP) analysis indicates that **1** contains 53.0 wt.-% Sn and 10.5 wt.-% P, in good agreement with the formula based on crystal-structure determination (calcd. 53.3 wt.-% Sn, 10.4 wt.-% P). This gives rise to an Sn/P ratio of 4:3. The elemental analysis showed that the C, H and N contents are 8.12, 1.70 and 3.16 wt.-% (calcd. 8.08 wt.-% C, 1.68 wt.-% H, 3.14 wt.-% N), respectively, corresponding to an empirical molar ratio of C/H/N = 6:17:2. These analysis results indicated that the solid sample of **1** was a pure phase.

The ICP analysis indicated that **2** contained 73.5 wt.-% Sn and 7.8 wt.-% P, in accordance with formula based on the single crystal structure analysis (calcd. 72.8 wt.-% Sn and 7.6 wt.-% P). The elemental analysis showed that it contained no C, H or N. These analytic results indicated that the solid sample of **2** was also a pure phase.

The FTIR spectrum of **1** was assigned as follows: The bands observed at 3505–3250 cm^{-1} were attributed to H-bonded N–H groups. The band at 2920 cm^{-1} was attributed to the δ_{C-H} vibration of 1,2-DACH. The bands 1109 and 965 cm^{-1} were assigned as the asymmetric stretching vibration of PO_4 units. Absorptions at 624, 536 and 486 cm^{-1} were due to bending vibration of PO_4 groups. The bands at 1624, 1559, 1540, 1446 and 1377 cm^{-1} were attributed to δ_{N-H}, ν_{C-H}, ν_{C-C} and ν_{C-N} vibrations of the doubly protonated 1,2-DACH cation occluded in the framework. The FTIR of **2** showed vibrations corresponding to the PO_4 unit at 1065, 1009, 600, 553 and 442 cm^{-1}.

Thermogravimetric analysis (TGA) curve showed that the weight loss of **1** occurring between 310 °C and 400 °C is 13.6%, and was related to the loss of absorbed water and the decomposition of the occluded amine (calcd. 12.8%). Differential thermal analysis (DTA) curve afforded a single broad endothermic peak at approximately 345 °C, corresponding to this decomposition. Similar analysis of **2** showed only a small mass loss (ca. 1.0%) at < 200 °C, due to the loss of absorbed water.

Description of the Structures

Detailed crystallographic data are listed in Table 1. and the selected bond lengths and angles are given in Table 2. The asymmetric unit of **1** is shown in Figure 1, (a). The structure of **1** shows the tin atom in a three-coordinate environment with respect to oxygen. The trigonal-pyramidal SnO_3 is alternatively linked to tetrahedral PO_4 units through bridging oxygen atoms. Of the eleven bridging oxygen atoms in the asymmetric unit, ten are bridged to a tin atom and a phosphorus atom. The remaining oxygen atom

Table 1. Crystallographic data and structure refinement parameters for $[Sn_4(PO_4)_3(OH)]^{2-}\cdot[trans\text{-}1,2\text{-}C_6H_{10}(NH_3)_2]^{2+}$ (**1**) and $(Sn_3O)_2(Sn_2O)(PO_4)_4$ (**2**).

	Compound **1**	Compound **2**
Chemical formula	$C_6H_{17}N_2O_{13}P_3Sn_4$	$O_{20}P_4Sn_{10}$
Crystal system	monoclinic	triclinic
Space group	$P2_1/n$ (No.14)	$P\bar{1}$ (No.2)
a [Å]	7.02494(14)	7.3400(15)
b [Å]	19.934(4)	7.5700(15)
c [Å]	14.215(3)	12.872(3)
α [°]	90	87.59(3)
β [°]	99.02(3)	85.77(3)
γ [°]	90	61.42(3)
V [Å^3]	2028.8(4)	626.3(2)
Z	4	1
F(000)	1656	720
Fw	892.87	1630.78
$\rho_{calcd.}$ [g cm^{-3}]	2.917	4.324
λ [Å]	0.71073	0.71073
T [K]	291(2)	293(2)
μ [mm^{-1}]	5.168	10.121
2θ range	3.54–55.00°	3.18–49.6°
Total data collected	7696	2196
Index ranges	$0 \le h \le 9$	$0 \le h \le 8$
	$-25 \le k \le 25$	$-7 \le k \le 8$
	$-18 \le l \le 18$	$-15 \le l \le 15$
Unique data	4354	1990
Observed data [$I > 2\sigma(I)$]	4075	1709
Refinement method	full-matrix least squares on F^2	full-matrix least squares on F^2
R Indexes [$I > 2\sigma(I)$]	R = 0.0422	R = 0.0350
	R_w = 0.1056	R_w = 0.0885
R Indexes (all data)	R = 0.0477	R = 0.0510
	R_w = 0.1087	R_w = 0.1297
Goodness of fit (S)	1.158	1.082
No. of parameters	264	155
Largest difference map peak and hole [e Å^{-3}]	0.988 and –1.221	2.211 and –1.911

 © 2007 Wiley-VCH Verlag GmbH & Co. KGaA, Weinheim

bonds two tin atoms. From the Fourier map, we note that the oxygen atom forming the Sn–O–Sn units is protonated. Bond valence sum calculations performed on the framework confirm the presence of the proton on the oxygen involved in forming the Sn–O(H)–Sn linkages.[10] Bonding involved two tin atoms and a hydroxy group has been previously reported.[5,11]

Table 2. Selected bond lengths [Å] and angles [°] for $[Sn_4(PO_4)_3(OH)]^{2-}\cdot[trans\text{-}1,2\text{-}C_6H_{10}(NH_3)_2]^{2+}$ (**1**).[a]

Sn(1)–O(5)	2.122(3)	P(2)–O(7)	1.520(4)
Sn(1)–O(10)	2.133(3)	P(2)–O(8)	1.541(3)
Sn(1)–O(4)	2.165(3)	P(2)–O(6)	1.553(3)
Sn(2)–O(13)	2.139(4)	P(2)–O(5)	1.560(3)
Sn(2)–O(1)	2.160(3)	P(3)–O(11)	1.518(4)
Sn(2)–O(6)[1]	2.193(3)	P(3)–O(10)	1.547(3)
Sn(3)–O(9)	2.132(3)	P(3)–O(9)	1.557(3)
Sn(3)–O(8)	2.153(3)	P(3)–O(12)	1.560(3)
Sn(3)–O(3)[2]	2.188(3)	O(2)–Sn(4)[4]	2.089(3)
Sn(4)–O(2)[3]	2.089(3)	O(3)–Sn(3)[5]	2.188(3)
Sn(4)–O(13)	2.109(4)	O(6)–Sn(2)[6]	2.193(3)
Sn(4)–O(12)	2.156(3)	N(1)–C(1)	1.504(6)
P(1)–O(2)	1.519(3)	N(2)–C(2)	1.501(6)
P(1)–O(4)	1.541(3)	C(1)–C(2)	1.506(9)
P(1)–O(3)	1.542(3)	C(1)–C(6)	1.521(8)
P(1)–O(1)	1.546(3)		
O(5)–Sn(1)–O(10)	89.98(12)	O(11)–P(3)–O(10)	113.9(2)
O(5)–Sn(1)–O(4)	86.17(13)	O(11)–P(3)–O(9)	106.6(2)
O(10)–Sn(1)–O(4)	83.33(13)	O(10)–P(3)–O(9)	110.49(19)
O(13)–Sn(2)–O(1)	85.54(14)	O(11)–P(3)–O(12)	110.9(2)
O(13)–Sn(2)–O(6)[1]	89.20(15)	O(10)–P(3)–O(12)	105.14(19)
O(1)–Sn(2)–O(6)[1]	85.20(12)	O(9)–P(3)–O(12)	110.7(2)
O(9)–Sn(3)–O(8)	89.68(13)	P(1)–O(1)–Sn(2)	135.12(18)
O(9)–Sn(3)–O(3)[2]	86.18(13)	P(1)–O(2)–Sn(4)[4]	140.43(2)
O(8)–Sn(3)–O(3)[2]	83.50(15)	P(1)–O(3)–Sn(3)[5]	127.6(2)
O(2)[3]–Sn(4)–O(13)	88.60(16)	P(1)–O(4)–Sn(1)	131.47(19)
O(2)[3]–Sn(4)–O(12)	86.60(13)	P(2)–O(5)–Sn(1)	109.94(18)
O(13)–Sn(4)–O(12)	89.47(15)	P(2)–O(6)–Sn(2)[6]	110.88(17)
O(2)–P(1)–O(4)	111.24(19)	P(2)–O(8)–Sn(3)	148.4(2)
O(2)–P(1)–O(3)	112.1(2)	P(3)–O(9)–Sn(3)	108.09(17)
O(4)–P(1)–O(3)	106.3(2)	P(3)–O(10)–Sn(1)	144.3(2)
O(2)–P(1)–O(1)	106.98(18)	P(3)–O(12)–Sn(4)	113.01(18)
O(4)–P(1)–O(1)	110.29(18)	Sn(4)–O(13)–Sn(2)	134.63(19)
O(3)–P(1)–O(1)	110.03(18)	N(1)–C(1)–C(6)	111.7(5)
O(7)–P(2)–O(8)	114.1(2)	N(1)–C(1)–C(2)	113.3(5)
O(7)–P(2)–O(6)	111.9(2)	C(2)–C(1)–C(6)	111.7(5)
O(8)–P(2)–O(6)	103.88(19)	N(2)–C(2)–C(1)	112.4(5)
O(7)–P(2)–O(5)	106.09(2)	N(2)–C(2)–C(3)	106.7(5)
O(8)–P(2)–O(5)	110.7(2)	C(1)–C(2)–C(3)	111.3(5)
O(6)–P(2)–O(5)	110.18(18)		

[a] Symmetry transformations used to generate equivalent atoms: 1: $x-1/2, -y+3/2, z-1/2$; 2: $x-1/2, -y+3/2, z+1/2$; 3: $x-1, y, z$; 4: $x+1, y, z$; 5: $x+1/2, -y+3/2, z-1/2$; 6: $x+1/2, -y+3/2, z+1/2$.

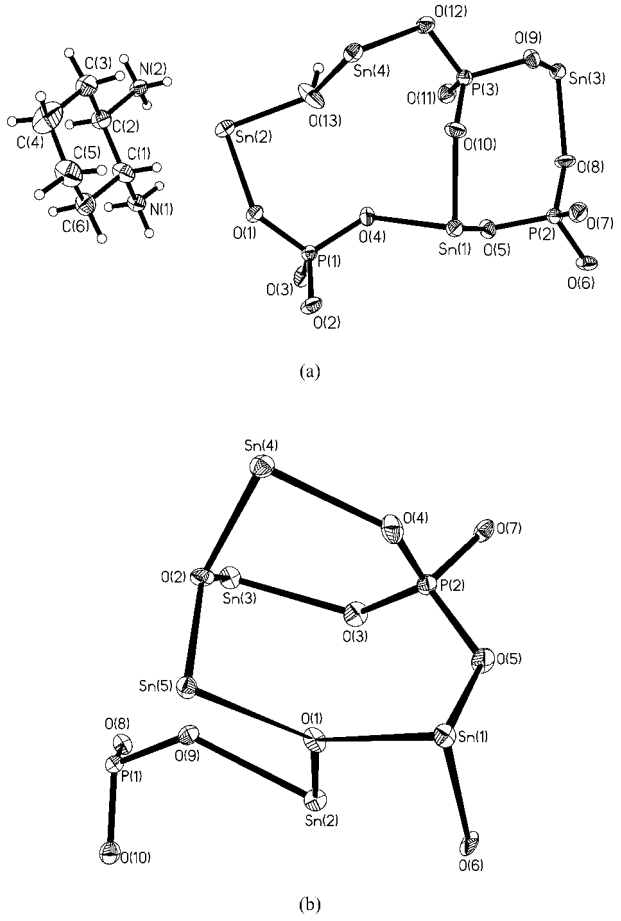

Figure 1. (a) ORTEP view of $[Sn_4(PO_4)_3(OH)]^{2-}\cdot[trans\text{-}1,2\text{-}C_6H_{10}(NH_3)_2]^{2+}$ structure showing the atom-labeling Scheme (30% thermal ellipsoids), with arbitrary radius of hydrogen atom. (b) ORTEP drawing of $(Sn_3O)_2(Sn_2O)(PO_4)_4$ structure showing the atom-labeling scheme (30% thermal ellipsoids).

There are two different phosphorus sites in the asymmetric unit of **1**. Of the three independent phosphorus atoms, P(1) atom is four-coordinate with respect to bridging oxygen (average P–O bond length 1.537 Å and average O–P–O bond angles 109.5°). P(2) and P(3) atoms are coordinated with three bridging oxygens and a double-bonded oxygen, respectively. The P(2)–O(7) distance of 1.520(4) Å and the P(3)–O(11) distance of 1.518(3) Å arise from the formal P=O double bond. The terminal P=O groups in $H_3PO_4\cdot0.5H_2O$, are generally between 1.485 and 1.495 Å in length.[12] The O–P–O bond angles are in the range 103.88–114.1° (av. 108.7°). The largest bond angle is observed for bonds involving the P=O linkage [114.1(1)° for P(2) and 113.7(2)° for P(3)], including the multiple-bond nature of P=O bonds. Each tin atom is triply coordinated to oxygen, resulting in average Sn–O bond length of 2.145 Å and average Sn–O bond angle of 86.93°. These values are in good agreement with other tin(II) phosphate open-framework structures.[5–7,13]

The connectivity of the PO_4 and SnO_3 units in **1** results in an anionic layer with the stoichiometry $[Sn_4(PO_4)_3(OH)]^{2-}$, which propagates along the *a*-axis. The structure is constructed entirely from a unit of double 5-rings.[14] Two 5-rings are joined each other through common edge of Sn–O–Sn to form the unit of two 5-rings. The units build up of zigzag chains through phosphorus bridges. These chains are related to one another by a center of inversion, and are linked in double-connected manner through oxygen bridges. The connection forms corrugated sheets along the *a* direction, resulting in 4-rings and 8-rings (Figure 2, a). The hydrogen atoms of the protonated *trans*-1,2-DACH molecules interact strongly with the framework oxygen atoms, espe-

 © 2007 Wiley-VCH Verlag GmbH & Co. KGaA, Weinheim

cially the doubly bonded ones. The organic amine molecules balance the charges of the anionic layers. Major hydrogen bonding interactions are presented in Table 3.

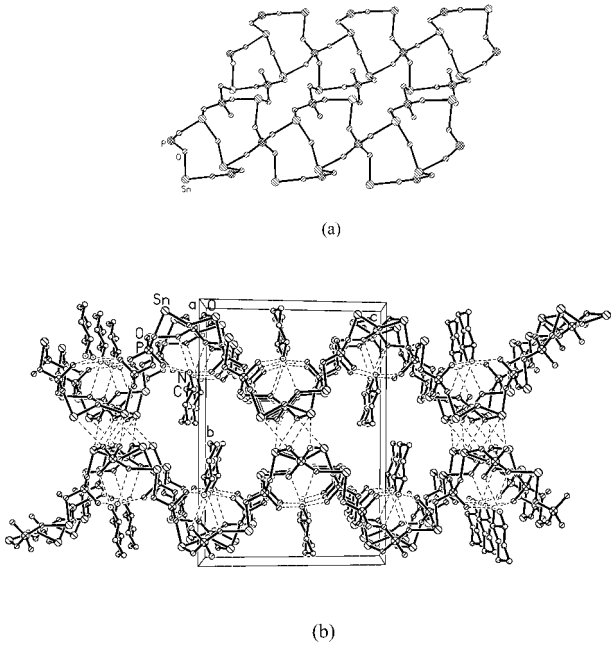

Figure 2. (a) Diagram of corrugated sheet along the *a*-axis, for compound **1**. (b) The structure of $[Sn_4(PO_4)_3(OH)]^{2-}$·[*trans*-1,2-$C_6H_{10}(NH_3)_2]^{2+}$ viewed along the *a*-axis, showing the pseudo 18-ring channels and the *trans*-1,2-diaminocyclohexane molecules (for clarity, hydrogen atoms are omitted).

Table 3. Important hydrogen bonds for $[Sn_4(PO_4)_3(OH)]^{2-}$·[*trans*-1,2-$C_6H_{10}(NH_3)_2]^{2+}$(**1**).

D–H	A	*d*(D–H)	*d*(D···H)	*d*(H···A)	DHA [°]
N1–H91A	O11	0.89	1.92	2.749(6)	154.1
N1–H91B	O3	0.89	2.10	2.815(5)	136.7
N1–H91C	O7	0.89	2.19	2.758(5)	121.0
N1–H91C	O9	0.89	2.45	3.137(5)	134.9
N2–H92A	O4	0.89	2.37	2.931(5)	121.6
N2–H92B	O11	0.89	2.28	2.876(6)	123.7
N2–H92B	O5	0.89	2.30	3.044(6)	141.4
N2–H92C	O7	0.89	1.89	2.752(5)	162.8

The bridging hydroxy groups in the framework are not involved in forming hydrogen bonds. The multipoint hydrogen-bonding interactions between amino groups and framework sheets cause the layers to bend. Presumably the two amino groups in *trans* configuration provide better access for hydrogen bond formation, compared to the *cis*-diamine. Thus, it afforded a more stable open-framework structure. This might be attributable to selective intercalation of *trans*-DACH with the exclusion of *cis*-DACH in compound **1**. This selectivity was confirmed by leaching experiments. The liquid residue obtained contained 98.9% *trans* diamine. The adjacent layers then are packed one over the other translated by approximately a one-half cell unit along the *c*-axis through the van der Waals interaction between tin atom and oxygen atom located in neighboring sheets (the distance between Sn and O is about 3.0 Å). This stacking leads to the formation of pseudo 18-ring channels along the *a*-axis (Figure 2, b). If van der Waals radii are taken into account, the width of 18-ring 1D channel is 1.62 nm × 1.26 nm (longest O–O distances and shortest O–O distances). The lone pair borne by the tin atom manifests itself in the lattice by creating open space in the channel. Repulsion between lone pairs associated with next tin atoms makes a small position shift between adjacent layers. At the same time, 8-ring channels are formed along the [011] direction.

An ORTEP representation of **2** is shown in part b of Figure 1 and the selected bond lengths and angles are given in Table 4. The tin atoms afford two different coordination environments with oxygen in this structure; the triply coordinated trigonal-pyramidal SnO_3 and the tetra-coordinated truncated square-pyramidal SnO_4. The SnO_3, SnO_4 and PO_4 moieties are vertex-linked forming the 3D neutral framework. The structure is dominated by a number of Sn_2O_2 4-rings, resulting in a higher Sn/P ratio (2.5), in con-

Table 4. Selected bond lengths [Å] and angles [°] for $(Sn_3O)_2(Sn_2O)(PO_4)_4$ (**2**).[a]

Sn(1)–O(5)	2.134(12)	Sn(5)–O(8)^3	2.322(11)
Sn(1)–O(1)	2.167(11)	P(1)–O(10)	1.532(13)
Sn(1)–O(6)	2.218(11)	P(1)–O(8)	1.569(11)
Sn(2)–O(1)	2.108(10)	P(1)–O(9)	1.592(13)
Sn(2)–O(10)^1	2.130(12)	P(1)–O(6)^4	1.616(11)
Sn(2)–O(9)	2.406(12)	P(2)–O(7)	1.552(12)
Sn(3)–O(2)	2.132(12)	P(2)–O(3)	1.575(13)
Sn(3)–O(7)^2	2.252(12)	P(2)–O(4)	1.584(13)
Sn(3)–O(3)	2.293(12)	P(2)–O(5)	1.598(12)
Sn(4)–O(2)	2.154(11)	O(6)–P(1)^5	1.616(11)
Sn(4)–O(4)	2.245(13)	O(7)–Sn(3)^2	2.252(12)
Sn(4)–O(7)^2	2.422(11)	O(7)–Sn(4)^2	2.422(11)
Sn(4)–O(8)^3	2.525(11)	O(8)–Sn(5)^6	2.322(11)
Sn(5)–O(2)	2.088(11)	O(8)–Sn(4)^6	2.525(11)
Sn(5)–O(1)	2.200(11)	O(10)–Sn(2)^1	2.130(12)
O(5)–Sn(1)–O(1)	89.1(4)	O(7)–P(2)–O(3)	110.4(7)
O(5)–Sn(1)–O(6)	83.7(5)	O(7)–P(2)–O(4)	108.0(7)
O(1)–Sn(1)–O(6)	83.8(4)	O(3)–P(2)–O(4)	110.3(7)
O(1)–Sn(2)–O(10)^1	84.2(4)	O(7)–P(2)–O(5)	106.1(7)
O(1)–Sn(2)–O(9)	80.1(4)	O(3)–P(2)–O(5)	112.2(7)
O(10)^1–Sn(2)–O(9)	85.4(4)	O(4)–P(2)–O(5)	109.7(7)
O(2)–Sn(3)–O(7)^2	74.8(4)	Sn(2)–O(1)–Sn(1)	114.9(5)
O(2)–Sn(3)–O(3)	87.2(4)	Sn(2)–O(1)–Sn(5)	117.6(5)
O(7)^2–Sn(3)–O(3)	88.4(4)	Sn(1)–O(1)–Sn(5)	127.4(5)
O(2)–Sn(4)–O(4)	89.7(4)	Sn(5)–O(2)–Sn(3)	127.4(6)
O(2)–Sn(4)–O(7)^2	71.0(4)	Sn(5)–O(2)–Sn(4)	112.3(5)
O(4)–Sn(4)–O(7)^2	85.4(4)	Sn(3)–O(2)–Sn(4)	111.5(5)
O(2)–Sn(4)–O(8)^3	74.3(4)	P(2)–O(3)–Sn(3)	135.1(7)
O(4)–Sn(4)–O(8)^3	77.7(4)	P(2)–O(4)–Sn(4)	137.0(7)
O(7)^2–Sn(4)–O(8)^3	141.3(4)	P(2)–O(5)–Sn(1)	118.5(7)
O(2)–Sn(5)–O(1)	94.6(4))	P(1)^5–O(6)–Sn(1	141.2(7)
O(2)–Sn(5)–O(8)^3	80.0(4)	P(2)–O(7)–Sn(3)^2	122.9(7)
O(1)–Sn(5)–O(8)^3	86.7(4)	P(2)–O(7)–Sn(4)^2	122.8(7)
O(10)–P(1)–O(8)	103.9(7)	Sn(3)^2–O(7)–Sn(4)^2	98.5(4)
O(10)–P(1)–O(9)	110.0(7)	P(1)–O(8)–Sn(5)^6	122.2(6)
O(8)–P(1)–O(9)	112.4(7)	P(1)–O(8)–Sn(4)^6	137.6(6)
O(10)–P(1)–O(6)^4	112.4(7)	Sn(5)^6–O(8)–Sn(4)^6	93.1(4)
O(8)–P(1)–O(6)^4	108.7(6)	P(1)–O(9)–Sn(2)	129.4(7)
O(9)–P(1)–O(6)^4	109.4(7)	P(1)–O(10)–Sn(2)^1	138.5(8)

[a] Symmetry transformations used to generate equivalent atoms: 1: $-x+1, -y+2, -z$; 2: $-x, -y+2, -z+1$; 3: $x-1, y, z$; 4: $x, y+1, z$; 5: $x, y-1, z$; 6: $x+1, y, z$.

 © 2007 Wiley-VCH Verlag GmbH & Co. KGaA, Weinheim

trast to those reported previously.[5–7,13] The triply-coordinated oxygen atoms do not create a situation where P–O–P bonding occurs, in accordance with Loewenstein rule.[15] Of the five independent Sn atoms in the asymmetric unit, Sn(1), Sn(2), Sn(3) and Sn(5) are triply-coordinated with respect to oxygen and the remaining Sn(4) atom is tetra-coordinated. The Sn(x)–O (x = 1, 2, 3, 5) bond lengths are in the range 2.088–2.406 Å (av. 2.336 Å), and the O–Sn(x)–O (x = 1, 2, 3, 5) bond angle are in the range 74.8–94.6° (av. 85.2°); The Sn(4)–O distances are in the range of 2.154–2.525 Å (av. 2.336 Å), and O–Sn(4)–O bond angles are in the range 71.0–141.3° (av. 89.9°). The longest Sn–O distance (2.525 Å) in the present structure as well as the largest O–Sn–O bond angle (141.3°) are associated with the tetra-coordinated Sn(4). P(1) and P(2) are both tetra-coordinate with respect to bridging oxygen with average P–O bond length of 1.577 Å and average O–P–O bond angle of 109.4°. These values are in agreement with those reported earlier.[5–7,13]

In the neutral framework structure **2**, the trigonal-pyramidal SnO_3, square-pyramidal SnO_4 and tetrahedral PO_4 units are linked through bridging oxygen atoms. The second building unit (SBU) is a cage that is composed of eight Sn atoms and two P atoms (Figure 3, a). These cages are linked through 4-rings (2P + 2Sn) in three different ways (Figure 3, b), i.e. connections between an oxygen atom of the cage and a phosphorus atom of the 4-ring, or between a tin atom of the cage and a phosphorus atom of the 4-ring through bridging oxygen atom, or between an oxygen atom of the cage, and a tin atom of the 4-ring. A 4-ring is connected with six cages. Each phosphorus atom of the 4-ring is linked with two cages, while each tin atom linked only with one cage. These cages are related to each other by a center of inversion diagonally in the 4-ring. In contrast, each cage is connected with six 4-rings, four of them through phosphorus atom of the 4-ring and the rest two through a tin atom of the 4-ring. These connections result in formation of 3D framework with sequences of helical 6-ring and elliptical 12-ring channels in the b-direction (Figure 3, b). A 6-ring consists of three phosphorus and three tin atoms, and 12-membered ring consists of four phosphorus and eight tin atoms. The maximal width of the channel is 9.37 Å (P–P distance, not including van der Waals radii). However, the minimal width is merely 0.5 Å (Sn–Sn distance, not including van der Waals radii). Since the lone pair borne by tin atom occupies the channels, access by any molecule is prohibited. Experiments of N_2 adsorption and desorption also verify this conclusion affording an adsorbed volume is only 4.29 $cm^3 g^{-1}$ at pressure of 790 Torr.

The framework density (FD) for **1** and **2** are 13.8 and 22.35 T-atoms (T = Sn, P) per nm^3, respectively. Compound **2** shows dense packing morphology compared to other framework materials (FD < 20).[14,16]

In conclusion, although a mixture of isomers of 1,2-DACH was used in the synthesis, only the *trans* species were as templates occluded in **1** as confirmed through leaching experiments. The *trans* isomer has two chiral centers, corresponding to 1*S*,2*S* and 1*R*,2*R* enantiomers. Four [*trans*-1,2-

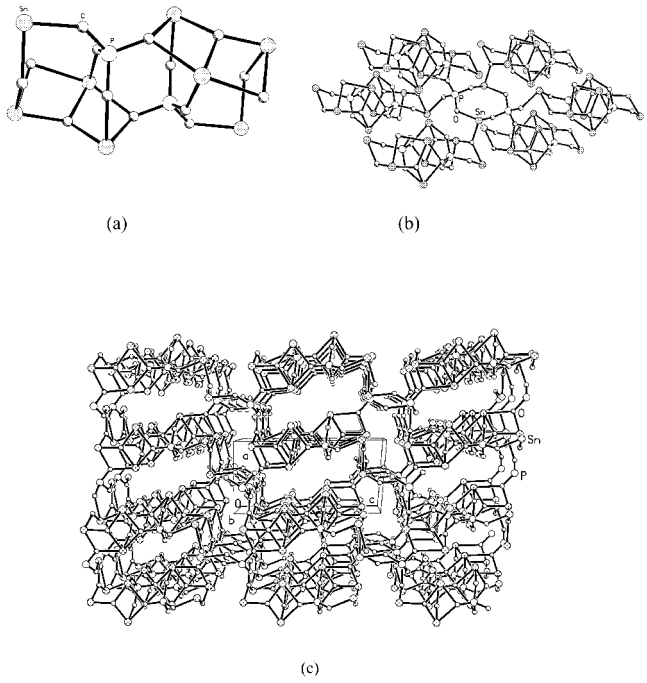

Figure 3. (a) Cage as a SUB for structure of compound **2**, $(Sn_3O)_2(Sn_2O)(PO_4)_4$. (b) The connections of cages with (2P + 2Sn) 4-ring. (c) The structure of $(Sn_3O)_2(Sn_2O)(PO_4)_4$ viewed along the *b*-axis, showing sequences of helical 6-rings and elliptical 12-rings channels in the same direction.

$C_6H_{10}(NH_3)_2]^{2+}$ cations are found in a unit cell and the nearest neighboring cations are symmetry related by a 2_1-screw axis (Figure 2, b). The cation site is occupied by mirror plane related diastereoisomer with an occupancy factor of 50%. When only *cis* isomer was used as template in the synthesis of **2**, no template molecule is occluded in the inorganic framework (Figure 3, c). Only a *trans* orientation of the two amino groups provides the appropriate hydrogen bonding interaction to result in complex formation. This may afford some interesting insight in terms of role that templates play in hydrothermal synthesis.

Experimental Section

Synthesis: All chemicals used were of analytical grade. Hydrothermal synthesis of **1** is described here. SnC_2O_4 (1.187 g, 5.74 mmol) was dispersed in 10 mL of water and 0.60 mL of 85 wt.-% aqueous H_3PO_4 was added to the mixture under continuous stirring. A mixture of *trans*- and *cis*-1,2-DACH (1.23 mL, 10 mmol) was added. The reaction mixture was stirred until it was homogeneous and the pH value was 7.4. The mixture (SnC_2O_4/1.5 H_3PO_4/1.8 DACH/58 H_2O) was transferred into a 23 mL Teflon™-lined stainless steel autoclave and heated at 443 K for 10 d under autogenous pressure. The pH value of the solution was 6.7. The solid product (in about 70% yield based on the Sn source) consisting of colorless schistose single crystals **1** was recovered by filtration, washed thoroughly with distilled water, and dried at room temperature. Compound **1** was also afforded with an approximate 60% yield when *trans*-1,2-DACH was used under the conditions. The pH values of the solution before and after reaction were 7.4 and 6.6, respectively. Colorless prismatic crystals of **2** were obtained hydrothermally using only

 © 2007 Wiley-VCH Verlag GmbH & Co. KGaA, Weinheim

cis-1,2-DACH as template under the same reaction conditions to those for **1**. The pH value of solution was 7.5 and the yield was about 58%.

Initial Characterization: The element analysis of the product was performed with a Foss Heraeus CHN-O-RAPID elemental analyzer, and the ICP analysis was performed with a Jarell-Ash 1100+2000 ICP instrument. The IR spectra were recorded with a Bruker 410 FT-IR spectrometer using KBr pellets. TGA and DTA were conducted with V1.1B TA thermogravimetric analyzer under nitrogen in the range between 25 and 600 °C, with a heating rate of 10 °C min^{-1}. Assays of isomeric residue in leaching experiment were carried out with a Varain-5000 high-performance chromatograph with fixed-wavelength UV absorbance detector set at 254 nm under ambient temperatures, on a 150 mm × 4.6 mm reversed-phase Eclipse XDB-C8 LC Column (Agilent Technologies Corp., USA) with an eluting mobile phase consisting of acetonitrile/0.05% phosphoric acid (45:55).

Single-Crystal X-ray Diffraction: A plate-like crystal of approximate dimensions 0.30 × 0.30 × 0.20 mm for **1** was mounted on a glass fiber on a Siemens Smart-CCD diffractometer equipped with graphite-monochromated Mo-K_α (λ = 0.71073 Å) radiation. A hemisphere of intensity data was collected at 291(2) K in the 2θ range 3.54–55.00°. A total of 4354 reflection was collected, of which 4075 were considered to be observed with $I > 2\sigma(I)$. Data processing was accomplished with SAINT processing program.[17] The structure was solved by direct methods and refined by full-matrix least-squares on F^2 using SHELX97.[18] Each carbon attached to an amino group is disordered with a SOF (site occupation factor) of 0.5. All non-hydrogen atoms were refined anisotropically. The hydrogen atoms were placed geometrically and allowed to ride on the atoms to which they were attached with fixed isotropic thermal parameters by program.

CCDC-165851 contains the supplementary crystallographic data of **1** for this paper. These data can be obtained free of charge from Cambridge Crystallographic Data Center at www.ccdc.cam.ac.uk/data_request/cif.

A prismatic crystal with dimension of 0.3 × 0.2 × 0.2 mm for **2** was mounted on a glass fiber. Data were collected on FR590 CAD-4 diffractometer (Mo-K_α radiation, λ = 0.71073 Å) at 293(2) K in the range $3.18 < 2\theta < 49.6°$ using the ω scan technique. A total of 1990 reflections were collected of which 1709 with $I > 2\sigma(I)$ were used. An empirical absorption correction was applied. The structure was solved by direct methods and refined using SHELX97 programs.[18] All atoms were refined anisotropically. Pertinent experimental details for the structure determination are listed in Table 1.

Further details of the crystal-structure investigation may be obtained from the Fachinformationszentrum Karlsruhe, 76344 Eggenstein-Leopoldshafen, Germany (http://www.fiz-karlsruhe.de), on quoting the depository number CSD-412358.

Leaching Experiment: Compound **1** (4.46 g, 5 mmol) was added to 50 mL of 0.2 N NaAc solution in THF. The mixture was continuously stirred under reflux for 10 h and cooled to room temperature. The solids were filtered off, washed with THF. Then 20 mL of 20% NaOH aqueous solution was added to the filtrate to liberate 1,2-DACH from the acetate salt. The mixture was continuously extracted with 40 mL of benzene for 5 h. The benzene extract was evaporated under vacuum, leaving a liquid residue (about 0.25 g, yield 44.0% based on the empirical formula of **1**). The liquid residue consisted of 98.9% *trans*-1,2-DACH and 1.1% *cis*-1,2-DACH.[19] After leaching, the crystal structure was lost and the resulting amorphous solid showed a different powder diffraction pattern from that of compound **1**.

Acknowledgments

The authors acknowledge the financial support from the Ministry of Science and Technology of China (Major State Basic Research Development Program, G 200077500).

[1] a) P. Y. Feng, X. H. Bu, G. D. Stucky, *Nature* **1997**, *388*, 737–741; b) S. Ekambaram, S. C. Sevov, *Angew. Chem. Int. Ed.* **1999**, *38*, 372–375; c) A. K. Cheetham, G. Ferey, T. Loiseau, *Angew. Chem. Int. Ed.* **1999**, *38*, 3269–3292; d) A. Choudhry, S. Neeraj, S. Natarajan, N. R. C. Rao, *J. Mater. Chem.* **2001**, *11*, 1537–1540; e) W. T. A. Harrison, M. L. F. Phillips, J. Stanchfield, T. M. Nenoff, *Inorg. Chem.* **2001**, *40*, 895–899.
[2] a) S. Natarajan, M. P. Attfield, A. K. Cheetham, *Angew. Chem., Int. Ed. Engl.* **1997**, *36*, 978–980; b) R. K. Chiang, *Inorg. Chem.* **2000**, *39*, 4985–4988; c) C. N. R. Rao, S. Natarajan, S. Neeraj, *J. Am. Chem. Soc.* **2000**, *122*, 2810–2817; d) S. H. Feng, R. R. Xu, *Acc. Chem. Res.* **2001**, *34*, 239–247.
[3] a) S. Natarajan, A. K. M. Eswaramoorthy Cheetham, C. N. R. Rao, *Chem. Commun.* **1998**, 1561–1562; b) S. Natarajan, A. K. Cheetham, *Chem. Commun.* **1997**, 1089–1090; c) G. Y. Yang, S. C. Sevov, *J. Am. Chem. Soc.* **1999**, *121*, 8389–8390.
[4] a) S. Natarajan, A. K. Cheetham, *J. Solid State Chem.* **1997**, *134*, 207–210; b) N. Stock, G. D. Stucky, A. K. Cheetham, *Chem. Commun.* **2000**, *22*, 2277–2278.
[5] S. Natarajan, S. Ayyapan, A. K. Cheetham, C. N. R. Rao, *Chem. Mater.* **1998**, *10*, 1627–1631.
[6] Y. L. Liu, S. Zhu, J. S. Chen, L. Y. Na, J. Hua, W. Q. Pang, R. R. Xu, *Inorg. Chem.* **2000**, *39*, 1820–1822, and references herein.
[7] a) A. Choudhry, S. Natarajan, C. N. R. Rao, *Inorg. Chem.* **2000**, *39*, 4295–4304; b) C. N. R. Rao, S. Natarajan, S. Neeraj, *J. Am. Chem. Soc.* **2000**, *122*, 2810–2817; c) P. Ramaswamy, S. Natarajan, *Eur. J. Inorg. Chem.* **2006**, 3463–3471.
[8] C. N. R. Rao, S. Natarajan, A. Choudhury, S. Neeraj, A. A. Ayi, *Acc. Chem. Res.* **2001**, *34*, 80–87.
[9] a) C. N. R. Rao, S. Natarajan, S. Neeraj, *J. Solid State Chem.* **2000**, *152*, 302–321; b) S. Neeraj, S. Natarajan, C. N. R. Rao, *Angew. Chem. Int. Ed.* **1999**, *38*, 3480–3483.
[10] I. D. Brown, D. Aldermatt, *Acta Crystallogr., Sect. B* **1985**, *41*, 244–247.
[11] T. H. Jordan, L. W. Schroeder, B. Dickens, W. E. Brown, *Inorg. Chem.* **1976**, *15*, 1810–1814.
[12] B. Dickens, E. Prince, L. W. Schroeder, T. H. Jordan, *Acta Crystallogr., Sect. B* **1974**, *30*, 1470–1473.
[13] a) S. Natarajan, M. P. Attfield, A. K. Cheetham, *Angew. Chem. Int. Ed. Engl.* **1997**, *36*, 978–980; b) S. Natarajan, A. K. Cheetham, *Chem. Commun.* **1997**, 1089–10900; c) N. Stock, G. D. Stucky, A. K. Cheetham, *Chem. Commun.* **2000**, 2277–2278; d) S. Natarajan, *J. Mater. Chem.* **1998**, *8*, 2757–2760.
[14] L. B. McCusker, *Comprehensive Supramolecular Chemistry*, vol. 7 (Eds.: G. Alberti, T. Bein), Pergamon, Oxford, **1996**, p. 393–422.
[15] W. Loewenstein, *Am. Mineral.* **1954**, *39*, 92–96.
[16] a) W. T. A. Harrison, *Chem. Mater.* **1996**, *8*, 145–151; b) C. H. Lin, S. L. Wang, K. H. Lii, *J. Am. Chem. Soc.* **2001**, *123*, 4649–4650.
[17] Software package SMART and SAINT, Siemens Analytical X-ray Instruments Inc., Madison, WI, **1996**.
[18] SHELXS 97, Siemens Industrial Automation Inc., **1997**.
[19] Samples of the residue were assayed on Varain-5000 high performance chromatograph with fixed-wavelength UV absorbance detector set at 254 nm. Samples (5 μL injection) were chromatographed at ambient temperatures on a 150 mm × 4.6 mm reversed-phase Eclipse XDB-C8 LC Column

 © 2007 Wiley-VCH Verlag GmbH & Co. KGaA, Weinheim

(Agilent Technologies Corp., USA) with an eluting mobile phase consisting of acetonitrile/0.05% phosphoric acid (45:55). Eluents were aspirated prior to use. At a flow-rate of 1.0 mL/min column equilibration with the mobile phase was achieved in approximately 30 min. The retention times are 8.6 min, 10.4 min, 11.9 min for *trans*-(1*S*,2*S*)-DACH, *cis*-1,2-DACH and *trans*-(1*R*,2*R*)-DACH, respectively. Samples preparation: 0.2 mL of 0.4% acetonitrile solution of 2,3,4,6-tetra-*O*-acetyl-D-glucopyranosyl isothiocyanate was added to 0.1 mL of 0.025% acetonitrile solution of 1,2-DACH. Ten minutes later, 0.1 mL of 0.2% acetonitrile solution of ethanolamine was added to the given mixture. And three minutes later, 2.0 mL of 0.05% phosphoric acid was added to dilute the above solution.

Received: September 27, 2006
Published Online: January 8, 2007

 © 2007 Wiley-VCH Verlag GmbH & Co. KGaA, Weinheim